Drug release from polymer-coated TiO_2 nanotubes on additively manufactured Ti-6Al-4V bone implants: a feasibility study

To cite this article: Chiara Micheletti *et al* 2021 *Nano Ex.* **2** 010018

NANO EXPRESS

PAPER

Drug release from polymer-coated TiO_2 nanotubes on additively manufactured Ti-6Al-4V bone implants: a feasibility study

Chiara Micheletti[1,2], **Raffaella Suriano**[1], **Kathryn Grandfield**[2,3] and **Stefano Turri**[1]

[1] Department of Chemistry, Materials and Chemical Engineering, Politecnico di Milano, Milan, Italy
[2] Department of Materials Science and Engineering, McMaster University, Hamilton, ON, Canada
[3] School of Biomedical Engineering, McMaster University, Hamilton, ON, Canada

E-mail: michelec@mcmaster.ca

Keywords: bone implant, SLM, titania nanotubes, surface topography, local drug delivery, polymer coating

OPEN ACCESS

RECEIVED
10 October 2020

REVISED
28 January 2021

ACCEPTED FOR PUBLICATION
2 February 2021

PUBLISHED
10 February 2021

Abstract

Insufficient osseointegration, inflammatory response and bacterial infection are responsible for the majority of bone implant failures. Drug-releasing implants subjected to adequate surface modification can concurrently address these challenges to improve the success of implant surgeries. This work investigates the use of Ti-6Al-4V (Ti64) with a dual-scale surface topography as a platform for local drug delivery. Dual-scale topography was obtained combining the inherent microscale roughness of the Ti64 samples manufactured by selective laser melting (SLM) with the nanoscale roughness of TiO_2 nanotubes (TNTs) obtained by subsequent electrochemical anodization at 60 V for 30 min. TNTs were loaded with a solution of penicillin-streptomycin, a common antibiotic, and drug release was tested in vitro. Three biocompatible and biodegradable polymers, i.e. chitosan, poly(ε-caprolactone) and poly(3-hydroxybutyrate), were deposited by spin coating, while preserving the microscale topography of the substrate underneath. The presence of polymer coatings overall modified the drug release pattern, as revealed by fitting of the experimental data with a power-law model. A slight extension in the overall duration of drug release (about 17% for a single layer and 33% for two layers of PCL and PHB) and reduced burst release was observed for all polymer-coated samples compared to uncoated, especially when two layers of coatings were applied.

1. Introduction

Titanium and its alloy Ti-6Al-4V (Ti64) are widely employed materials for orthopaedic and dental implants due to their high excellent biocompatibility and corrosion resistance provided by the thin oxide layer (TiO_2, also termed titania) that spontaneously forms on their surface [1]. This surface oxide layer is also considered responsible for the bioactivity of titanium-based implants and hence their natural ability to osseointegrate [2, 3].

Successful osseointegration, i.e. the formation of a structural and functional connection between implant and the host bone tissue [4], relies on several aspects, among which surface topography has been shown to play an important role [5]. In particular, several studies have concluded that microscale topography can improve osseointegration [6, 7]. Recently, the processability of titanium alloys by selective laser melting (SLM), an additive manufacturing (AM) technique, has emerged as a method to obtain parts with an inherent microrough surface without subsequent post-processing steps. Such microroughness is conferred by the presence of randomly distributed microspherical particles on the surface as a result of unmelted and unsintered process powders [8] and balling effects [9]. Moreover, AM components can be highly customized, hence patient-specific bone implants can be fabricated.

Not only microscale, but also nanoscale roughness has been shown to be beneficial for osseointegration [10]. Among the several strategies to produce nanoscale features, a well-investigated possibility is the generation of well-ordered arrays of TiO_2 nanotubes (TNTs) by electrochemical anodization [11]. TNTs have demonstrated excellent biocompatibility and cell responses *in vitro* [12]. Furthermore, promising results in terms of improved osseointegration have been obtained *in vivo* [13].

Not only are TNTs believed to be beneficial for osseointegration, but they could also serve as platforms for local drug delivery [14, 15]. In addition to insufficient osseointegration, other factors still pose challenges to the success of bone implants, i.e. inflammatory responses and bacterial infections. Treatments for reducing the risk of inflammation and infection post-surgery currently involve systemic administration of inflammatory drugs and antibiotics, respectively. However, conventional systemic drug therapy in bone presents some limitations, including low efficacy, lack of selectivity, poor bioavailabilty and biodistribution, and toxicity [14]. While drug delivery to specific skeletal sites remains challenging, drug-releasing bone implants have emerged as a possibility to overcome the limitation of conventional drug administration [14, 16, 17]. In fact, thanks to local drug delivery, site-specific and optimal drug concentration can be achieved, without dilution across the entire body, hence leaving other sites unaffected and avoiding toxicity and side effects. Given their hollow nature, (nano) tubes closed at the bottom and open at the top, therapeutic agents can be accommodated inside the TNTs. Drug release kinetics and overall duration are influenced by the nanotube size [18], which in turn can be adjusted by the electrochemical anodization process parameters (e.g. anodization time and voltage) [19]. Different strategies to control and extend the drug release have been proposed, including the use of polymer coatings to cap the nanotube top opening [20–22].

Electrochemical anodization of SLM substrates was first proposed by Gulati *et al* to combine the inherent microscale topography of SLM parts and the nanoscale of the TNTs [23]. The resulting dual-scale surface topography can benefit from both microscale and nanoscale in improving osseointegration [10]. Moreover, the viability of this type of substrate for local drug delivery has been tested *in vitro* [24].

In this work, the possibility to employ drug-releasing bone implants with a dual-scale surface topography was further investigated. Ti64 samples were manufactured by SLM and electrochemically anodized to generate TNTs on their surface. The release of the model antibiotic drug penicillin-streptomycin (pen-strep) loaded in the TNTs was assessed *in vitro*. This paper presents several new approaches not previously investigated. First, our work is the first example of drug release from polymer-coated TiO_2 nanotubes on SLM substrates, aiming to combine the benefits of antibacterial capabilities and enhanced osseointegration thanks to drugs delivered from a surface with nano- and microscale features. While previous studies have investigated the use of polymer coatings to control drug release duration and kinetics from TNTs on flat samples [20–22, 25], this has never been examined for samples with a dual-scale surface topography. Second, two biodegradable polyesters never employed in local drug delivery studies with TNTs, i.e. poly(ε-caprolactone) (PCL) and poly(3-hydroxybutyrate) (PHB), were used. These were compared to the more commonly employed chitosan. Third, while most studies employ dip coating [20–22], in our work spin coating was used instead to deposit the polymer coatings. Fourth, we examined the drug release pattern by fitting with the Korsmeyer-Peppas's power law model to compare the diffusion behaviour of uncoated and coated TNTs. Both single- and double-coated nanotubes were investigated to evaluate the role of coating thickness on drug release. Surface topography and morphology, roughness and wettability were characterized for uncoated and coated substrates.

2. Materials and methods

2.1. Fabrication of Ti64 samples with dual-scale surface topography

Ti64 samples with a dual-scale surface topography were obtained combining SLM and electrochemical anodization as previously described [26]. Briefly, Ti64 samples were manufactured by SLM (EOSINT M280 machine, EOS GmbH, Munich, Germany) as 10 mm $\times$ 10 mm $\times$ 1 mm squares with a 3 mm $\times$ 10 mm $\times$ 1 mm handle. The samples were then electrochemically anodized at 60 V for 30 min by immersing their square portion in a solution of ethylene glycol (certified grade, Sigma Aldrich) with 0.3% (w/w) of ammonium fluoride (certified grade, Fisher Chemical) and 2% (v/v) of deionized water, under mild magnetic stirring. Afterwards, they were ultrasonicated for 30 s in ethanol. The handle was then detached from the square base and discarded. The specimens were tested as-printed in this study, without heat treatment prior or post anodization.

2.2. Drug loading

After rinsing in acetone and drying, anodized Ti64 samples were plasma treated for 60 s with atmospheric air using a plasma system (Kenosistec Srl, Perugia, Italy) operated at a power of 150 W, to ensure high surface hydrophilicity and facilitate drug loading. Afterwards, a solution of pen-strep (10000 IU ml^{-1} of penicillin and 10 mg ml^{-1} of streptomycin, Sigma Aldrich) was loaded in the samples by progressively drop casting 5 μl of pen-strep solution until 1 ml of antibiotic solution was loaded. The sample surface was allowed to dry in air in between subsequent loading steps. Samples were then gently rinsed with phosphate-buffered saline (PBS) (Sigma Aldrich; pH = 7.4) to remove any surface-bound drug and allowed to dry in air at room temperature.

2.3. Preparation of polymer solutions and spin coating

Chitosan powder (molecular weight 50,000–190,000 Da, degree of deacetylation 75%–85%, Sigma Aldrich) was dissolved at 2% (w/v) in 0.8% (v/v) of acetic acid (glacial, Sigma Aldrich) and distilled water. PCL pellets (number average molecular weight 80000, Sigma Aldrich) was dissolved at 5% (w/w) in chloroform (analytical reagent grade, Fisher Chemical). PHB pellets (P209, Biomer) was dissolved at 4% (w/v) in chloroform (analytical reagent grade, Fisher Chemical) at 50 °C under magnetic stirring. The PHB-based solution was then centrifugated at 3500 rpm for 45 min (Rotofix 32A centrifuge, Hettich, Beverly, USA).

150 μl of polymer solution of either chitosan, PCL or PHB, was deposited on the surface of drug-loaded samples, and they were subsequently spin coated for 15 s (WS-400BZ-6NPP/LITE spin coater, Laurell Technologies Corp., North Wales, USA). Spin coating angular velocity was set to 500 rpm for chitosan, 500 rpm for PHB and 5000 rpm for PCL. Once dry, some samples were spin coated a second time with 150 μl of the same polymer solution and process parameters used for the first coating layer.

2.4. Characterization of uncoated and coated substrates

Surface morphology and topography of the SLM Ti64 samples before and after anodization was imaged with scanning electron microscopy (SEM) (JSM-7000F SEM, JEOL, Peabody, USA). Average size of the microspherical particles of the SLM samples and average TNT diameter of the anodized sample was measured from the SEM micrographs using ImageJ (NIH, Bethesda, USA). More details on how these measurements were carried out are provided in our previous work [26]. SEM was also used to collect both secondary electron (SE) and backscattered electron (BSE) images of spin coated samples (EVO 50 SEM, Zeiss, Jena, Germany). Coating thickness was estimated from mass variation before and after spin coating, assuming that the coating material was homogeneously distributed on the substrate. To better account for the surface roughness, the 'true' surface area was estimated from the geometrical area of the sample by means of the developed interfacial area ratio (S_{dr}). S_{dr} was measured using a focus variation instrument (Alicona Infinite Focus G5, Alicona Imaging GmbH, Graz, Austria), averaging the values of S_{dr} obtained for three different samples. Surface roughness of anodized and single-coated samples was evaluated by laser profilometry (UBM Microfocus, UBM Messtechnik GmbH, Ettlingen, Germany). Linear roughness parameters (e.g. R_a, R_q, R_z) were measured in three different spots per sample and the values obtained were statistically averaged. Both evaluation of coating thickness and surface roughness were repeated in duplicates, and results were statistically averaged. Hydrophilicity of polymer coatings was evaluated by measuring the water contact angle (OCA 20, DataPhysics Instruments GmbH, Filderstadt, Germany) in triplicates using two single-coated samples per coating material. From the measured water contact angles, values of equilibrium (Young) contact angle were obtained by applying the Wenzel's model for homogeneous wetting [27], in order to take into account the surface roughness. The roughness factor (r) in the Wenzel's model was computed from S_{dr} ($r = 1 + S_{dr}$ [28]). Roughness and wettability were assessed for single-coated samples only, and it is assumed these properties were not significantly affected by the presence of a second coating layer.

2.5. Characterization of drug release

Drug-loaded uncoated and spin coated (one or two coating layers of chitosan, PCL and PHB) were immersed in 1 ml of PBS and incubated at 37 °C. Every 20 min, 200 μl of release medium was withdrawn and replaced with fresh PBS. Subsequently, 20 μl of each withdrawn sample was mixed with 200 μl of BCA working reagent (Pierce BCA protein assay kit, ThermoFisher) in a 96-well plate and incubated at 37 °C for 30 min. Absorbance was measured at 570 nm with a microplate reader (GENios Plus, Tecan, Männedorf, Switzerland) and the corresponding pen-strep concentration was quantified using a calibration curve previously constructed for pen-strep. Absorbance was measured for two withdrawn samples per release time point for each sample, and the absorbance values were statistically averaged, after subtraction of blank (100% PBS) absorbance. The cumulative drug release was obtained by dividing the amount of drug released at a given time by the total amount of drug released. Two samples per type (uncoated; chitosan-, PCL- and PHB-coated; single and double coatings) were used to test the drug release, and the values of cumulative drug release obtained for the two samples were statistically averaged. Finally, the cumulative drug release profile was fitted using the Korsmeyer-Peppas's power law model, i.e. $M_t/M_\infty = kt^n$ ($M_t/M_\infty =$ fraction of drug released at time t, $k =$ release rate constant, $n =$ release exponent) [18, 29, 30], using OriginPro 8 (OriginLab Corporation, Northampton, USA). Only the experimental data up to a cumulative release around 80% were considered for the fitting, in order to exclude the plateau-like region from this analysis. Statistical significance in cumulative drug release at fixed time intervals for different groups was determined using a one-way ANOVA with a post-hoc Tukey's HSD test ($\alpha = 0.05$).

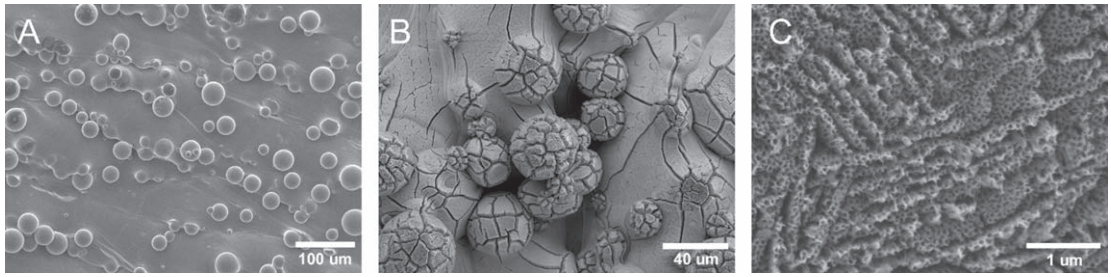

Figure 1. SEM images of the surface of Ti64 samples before (A) and after (B), (C) electrochemical anodization. (A) reveals the spherical microparticles characteristic of manufacturing by SLM. (B) shows the typical cracks appearing on the surface of the samples after anodization: these cracks are attributed to the formation of separate arrays of TNTs growing on curved surfaces (more details about anodization and cracks formation can be found in [31]). (C) provides a zoomed-in view of one of the well-ordered arrays of TNTs present in (B).

Table 1. Values of coating thickness for single and double coatings of chitosan, PHB and PCL. Spin coating angular velocities employed are also reported.

Coating	Coating thickness [μm]	Spin coating angular velocity [rpm]
Chitosan—one layer	2.0 ± 0.2	500
Chitosan—two layers	3.6 ± 0.2	500
PHB—one layer	2.5 ± 0.2	500
PHB—two layers	5.1 ± 0.2	500
PCL—one layer	1.4 ± 0.4	5000
PCL—two layers	2.9 ± 0.2	5000

3. Results

3.1. Dual-scale surface topography

Ti64 samples manufactured by SLM showed the presence of microspherical particles on the surface characteristic of this AM process (figure 1(A)). These microparticles had an average diameter of 26 μm. Imaging by SEM of the SLM Ti64 samples after anodization confirmed the presence of TNTs on both the microparticles and the flatter areas of the samples, and thus the creation of a dual-scale surface topography (figures 1(B)–(C)). In this work, TNTs with a diameter of around 70 nm were obtained. Comprehensive characterization of Ti64 samples with a dual-scale surface topography, including TNT diameter calculation and high-resolution SEM images, is available in our previous work [26].

3.2. Polymer coatings

Samples were successfully spin coated with one or two layers of chitosan, PCL and PHB. Table 1 reports the values of coating thickness estimated by mass variation for the three polymers for both single and double spin coatings. A roughly two-fold increase in coating thickness was obtained with the second spin coating step, as expected.

From SE imaging in SEM, chitosan and PCL coatings appeared to be uniform and homogeneous, while PHB coating displayed higher porosity and heterogeneity (figure 2). The presence of brighter regions in the BSE images of PCL coatings compared to chitosan coatings (figure 2) may indicate detection of more signal from the Ti substrate underneath. This suggests a lower thickness of PCL coatings compared to chitosan coatings, confirming what was assessed by the measurement of coating thickness (table 1). PHB coatings appeared less uniform from BSE imaging, supporting the film heterogeneity observed in the SE images (figure 2). Overall, SEM images indicated that the polymer coatings tended to reproduce the morphology and topography of the underlying substrate. This was further confirmed by measurement of surface roughness, as coated samples displayed roughness values analogous to the uncoated ones (table 2).

Chitosan coatings resulted in a slightly hydrophilic surface, as an average water contact angle of (89.7 ± 10.3)° was obtained. Both PHB and PCL coatings appeared to be more hydrophobic, with water contact angles equal to (107.5 ± 8.4)° and (96.5 ± 8.7)°, respectively. These values of equilibrium contact angle

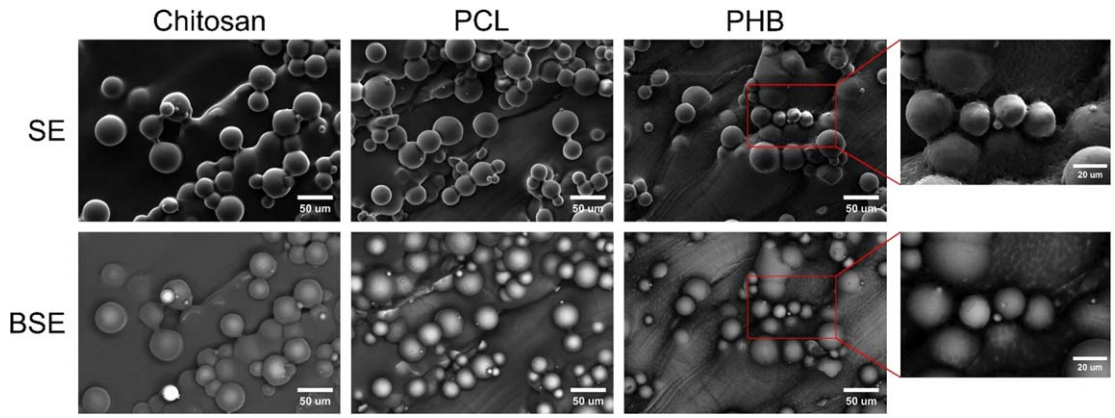

Figure 2. SE and BSE images of chitosan, PCL and PHB coatings deposited on SLM Ti64 samples by spin coating. While chitosan and PCL coatings appeared homogeneous, higher porosity was observed for PHB coatings in SE images (top inset), and a more heterogeneous BSE signals was also collected (bottom inset).

Table 2. Values of R_a, R_q and R_z roughness parameters for uncoated and single-coated Ti64 samples as measured by laser profilometry.

	R_a [μm]	R_q [μm]	R_z [μm]
Uncoated	7.0 ± 0.5	8.6 ± 0.7	37.8 ± 3.9
Chitosan-coated	6.1 ± 0.5	7.6 ± 0.5	33.6 ± 2.7
PHB-coated	7.2 ± 0.7	8.7 ± 0.9	37.7 ± 2.9
PCL-coated	7.0 ± 0.3	8.6 ± 0.5	36.8 ± 3.1

(Young) were computed by applying the Wenzel's model for homogeneous wetting [27] to the water contact angles measured experimentally. The roughness ratio in Wenzel's equation was computed considering an average S_{dr} of 186%, which was determined by focus variation. All the coatings led to a significant decrease in wettability compared to uncoated samples, which displayed a super-hydrophilic behaviour (contact angle close to 0°) after air plasma treatment.

3.3. Drug release

A drug release profile from uncoated samples is shown in figure 3. Drug release lasted a total of four hours and was characterized by an initial burst release, as 90% of pen-strep was released in the first 120 min.

A slightly more extended drug release was obtained for single-coated samples (figure 4). In particular, a total drug release time of 280 min was reached with chitosan coatings. Drug release time was extended to 300 min for both PCL- and PHB-coated samples. Therefore, an increase in the release time equal to about 8% and 17% was registered using chitosan and both PCL and PHB, respectively. Use of a second coating layer allowed for further increase in the total duration of drug release (figure 4). In fact, for double-coated samples, drug release lasted 300 min in presence of chitosan coatings, and 320 min with both PCL and PHB coatings. Therefore, compared to uncoated substrates, the increase in drug release time was approximately equal to 17% for chitosan and 33% for PCL and PHB double coatings.

Both single- and double- coated samples displayed a release pattern analogous to uncoated samples, with an initial burst release followed by a slower release stage, until reaching a plateau. However, the initial burst release was reduced by the presence of coatings, as can be seen from the bar graph in figure 5. In particular, the reduction in burst release was more significant in the first 60 min, while over time the cumulative drug release from coated samples tended to reach the same value as for the uncoated ones. Among single-coated samples, those with chitosan exhibited the highest decrease in initial drug release, as 20% less pen-strep was released in the first 60 min compared to uncoated substrates. This reduction in initial drug release became equal to 28% when using two layers of chitosan, which was statistically significant (Tukey's HSD, $p < 0.05$). PCL coatings reduced the amount of pen-strep released in the first hour by 16% and 19% for single and double coatings, respectively, compared to uncoated samples. For PHB single-coated samples, 8% less antibiotic was released in the first 60 min compared to uncoated substrates, while a statistically significant reduction equal to 24% was obtained when using double-coated samples (Tukey's HSD, $p < 0.05$).

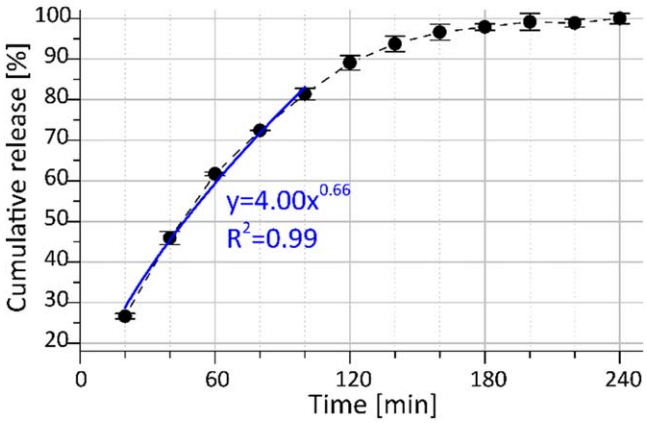

Figure 3. Cumulative drug release from uncoated samples. The blue line represents the power law fitting of the experimental data. The equation resulting from this fitting is reported on the graph in the form $y = kx^n$, where y corresponds to the cumulative drug release (M_t/M_∞ in the Korsmeyer-Peppas model) and x represents time.

Power law fitting using the Korsmeyer-Peppas model [29, 30] revealed a non-Fickian release behaviour for all the groups, as values of the release exponent (*n*) were greater than 0.5 (Fickian diffusion) [32]. This deviation was more pronounced for both single- and double- coated samples, compared to uncoated nanotubes, as greater values of *n* were obtained when polymer coatings were present (fitting equations are reported on the graphs in figures 3 and 4 for uncoated and coated samples, respectively).

4. Discussion

4.1. Dual-scale surface topography

Samples with a dual-scale topography were obtained by combining the inherent microscale of parts produced by SLM with the nanoscale features of TNTs generated by electrochemical anodization (figure 1), using the approach first proposed by Gulati *et al* [23], but employing different anodization conditions (electrolyte, time and voltage) already tested in our previous work [26]. This method is considered a promising strategy to improve osseointegration of Ti-based bone implants, as both microscale and nanoscale topography have been proved to be beneficial to this regard [10]. Moreover, this method combines the merits of both AM and electrochemical anodization. In fact, the use of AM processes, such as SLM, offers high customization since samples of any size and shape can be manufactured considering each patient's specific needs [33, 34]. On the other hand, electrochemical anodization is a facile approach to obtain TNTs and to easily tune their diameter and length by adjusting the process parameters (e.g. anodization time and voltage) [11, 19].

4.2. Polymer coatings

Three biocompatible polymers, i.e. chitosan, PCL and PHB, were successfully deposited on the SLM and anodized Ti64 samples by spin coating (figure 2). Dip coating and plasma polymerization have been previously investigated as methods to polymer-coat nanoporous structures [21, 35]. Although spin coating is more commonly employed with planar substrates [36], it was identified as an easy and effective approach to deposit polymer coatings on TNTs, despite the roughness of the substrate underneath. In the spin coating process, coating thickness depends on solution concentration (viscosity) and spin coating angular velocity [37]. To compensate for the different viscosities displayed by the solutions of chitosan, PCL and PHB, different spin coating angular velocities were employed, which in turn produced coatings with comparable thicknesses in the range of few μm (table 1).

The microscale surface topography of the SLM substrates was preserved by the polymer coatings, which tended to reproduce the morphology of the substrate underneath, as indicated by the comparable roughness values measured by laser profilometry (table 2). This is an important aspect to consider for the potential use of these substrates as bone implants, as microscale surface topography has been shown to improve osseointegration [6, 7]. On the other hand, the presence of the polymer coatings may mask the nanoscale surface topography created by the anodized TNTs. However, this shall be regarded as a temporary limitation, as polymer

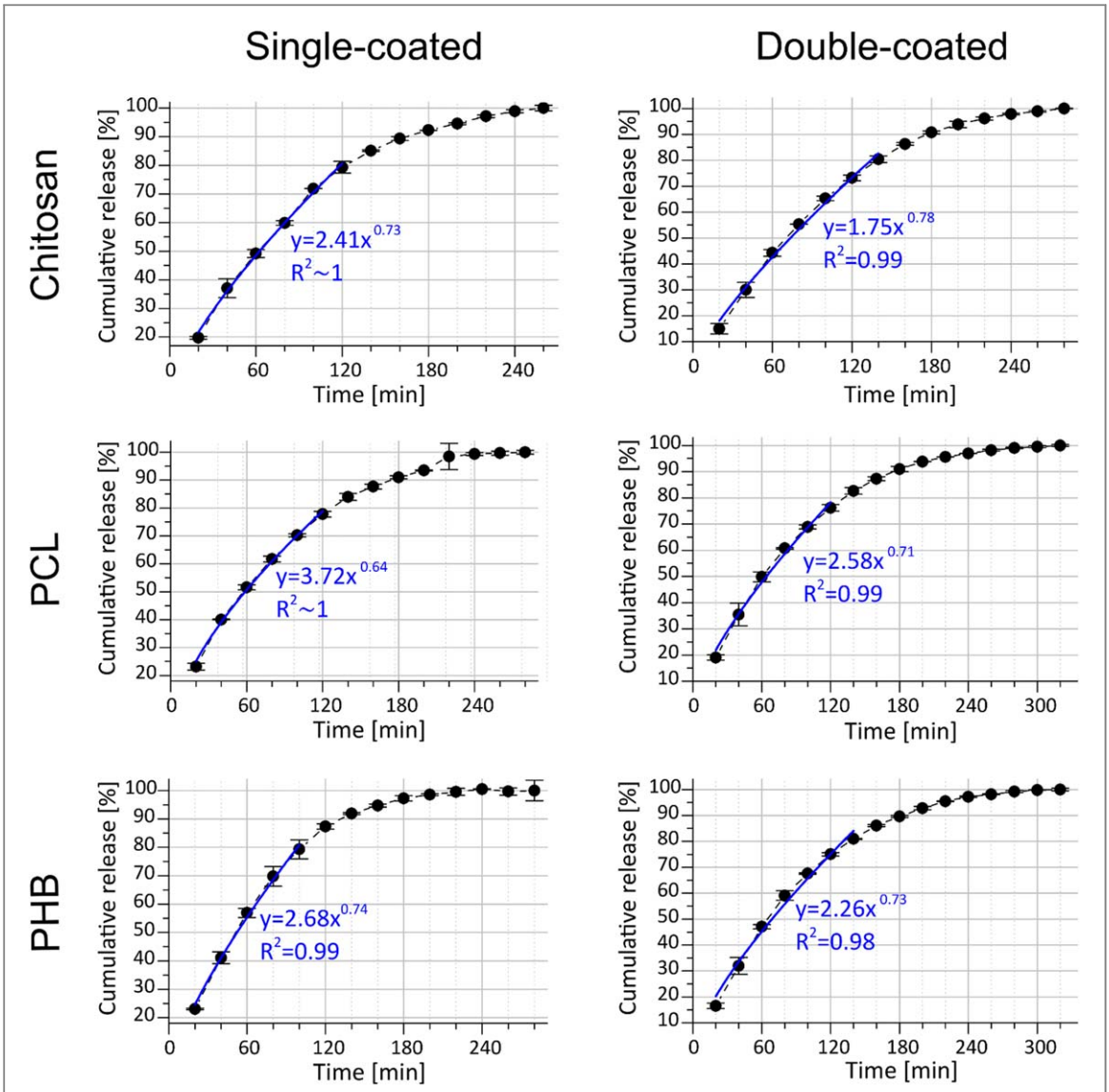

Figure 4. Cumulative drug release from samples coated with one (left) or two (right) layers of chitosan, PCL and PHB. The blue lines represent the power law fitting of the experimental data. The equation resulting from this fitting is reported on the graph in the form $y = kx^n$, where y corresponds to the cumulative drug release (M_t/M_∞ in the Korsmeyer-Peppas model) and x represents time.

coatings would eventually degrade over time, unveiling the dual-scale surface topography, which, therefore, could contribute to long-term osseointegration.

While chitosan coatings displayed hydrophilic properties, PHB and PCL resulted in slightly hydrophobic surfaces. This may limit their application as coatings for bone implants, as hydrophilic surfaces have been shown to better promote the initial biological cascade that ultimately leads to osseointegration [28]. However, hydrophilicity of PHB and PCL could be improved by, for example, functionalization or copolymerization [38, 39].

4.3. Drug release

As dual-scale surface topography has shown promising results for improved osseointegration, the use of this type of substrates as local drug delivery platforms could further enhance their potential as bone implants. Although the potential of TiO_2 nanotubes for local drug delivery has been intensively investigated [14, 15, 18], studies have been limited to flat Ti substrates and little attention has been paid to using samples with a dual-scale surface topography. In fact, to our knowledge, only one attempt has been reported [24]. Our study further investigates this possibility and, for the first time for this type of substrate, explores the use of polymer coatings to modify the drug release pattern.

TNTs nanotubes were successfully loaded with pen-strep, a commonly used antibiotic. Drug release lasted a total of 4 h (figure 3), which is significantly shorter than what was obtained in a study by Maher *et al* where vancomycin was released for 5 days from nanotubes on samples with analogous dual-scale surface topography [24]. Other studies using TNTs on flat Ti substrates have achieved drug release of different time length, spanning

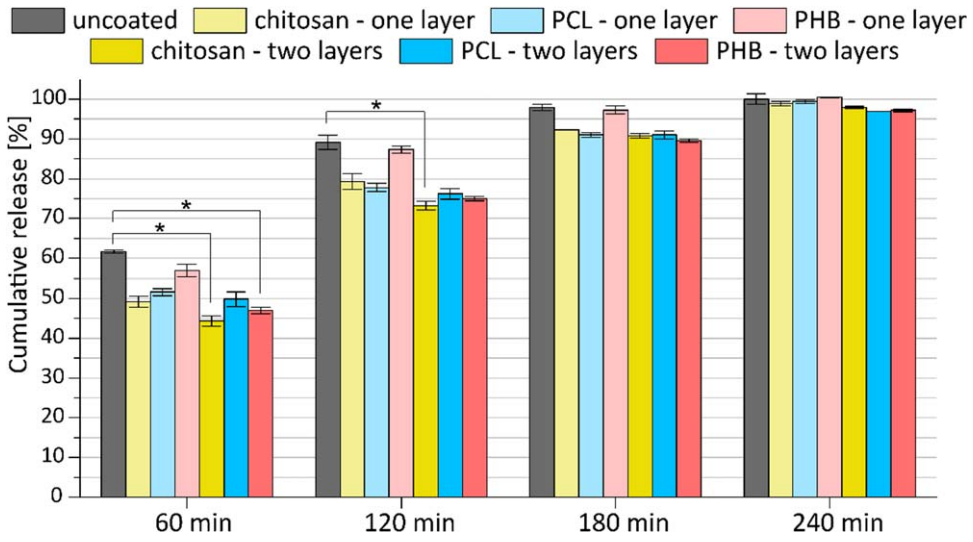

Figure 5. Bar chart representing the cumulative drug release from uncoated, single-coated and double-coated samples at fixed time intervals, i.e. 60 min, 120 min, 180 min and 240 min. It can be noticed that coatings reduced the amount of drug released compared to uncoated samples in the earlier time points. * indicates statistical significance ($p < 0.05$).

from 30 min [25] to up to 24 days [18]. Drug release from nanotubes is a diffusion-based process controlled by several factors including the dimension of the nanotubes (diameter and length), their surface chemistry, the molecular size and charge of the drug, the interfacial interaction between nanotube surface and drug molecules, the diffusion coefficient and dissolution rate of the drug, and the pH [15]. Therefore, different results obtained in different studies can be attributed to the variability in experimental conditions (e.g. nanotube dimensions, drug used, etc) adopted. In agreement with what commonly observed, drug release was characterized by an initial burst release, which is believed to be a consequence of the high concentration gradient at the drug-solution interface and the rapid diffusion of the drug molecules at the top end of the nanotubes [14], [40].

Coating of TNTs with polymers is considered a promising strategy to reduce the initial burst release and achieve a more prolonged and sustained drug release over time, as they reduce or completely cap the nanotube opening at the top surface and hence act as a physical barrier at the drug-solution interface [14, 15, 22]. Chitosan and poly (lactic-co-glycolic acid) (PLGA) have already shown promising results in extending the overall drug release compared to uncoated TNTs for flat Ti substrates [20–22, 25]. In this work, we evaluated the effectiveness of this strategy for samples with a dual-scale surface topography using chitosan, which has already been investigated in similar applications [20–22], and PHB and PCL, which instead have never been employed for this scope. Both PCL and PHB display relatively slow degradation rates compared to other biodegradable polyesters [41, 42], which could be beneficial to ensure presence of the coating and hence hinder the drug release over an extended period of time.

Chitosan, PHB and PCL coatings made it possible to extend the drug release compared to uncoated substrate (figure 4). As anticipated, drug release was longer for double-coated than single-coated nanotubes, as the thicker the coating, the more pronounced the barrier effect to the diffusion of the drug molecules is [21]. Independently of the number of coating layers, drug release was longer for nanotubes coated with PHB and PCL compared to chitosan. This could be attributed to the different interfacial properties in terms of hydrophilicity/hydrophobicity: as chitosan was more hydrophilic, it could be more permeable to the water-soluble pen-strep, as opposed to the more hydrophobic PCL and PHB. As drug release also depends on the relationship between drug molecular size and polymer structure (e.g. pore size), this aspect should be better investigated to assess the different behaviour of the three polymers employed, specifically in order to estimate the diffusion coefficient [43]. In addition, penetration of pen-strep inside the nanotubes and its diffusion outwards could be further examined, for example by comparing it to drug release from SLM samples without TNTs (i.e. not anodized), both without and with polymer coatings in the future. In particular, this could shed light on the rapid initial burst release.

The initial burst release was reduced for all the polymer coatings and thicknesses tested, as less antibiotic was released from polymer-coated substrates compared to uncoated ones, especially in the first 60 min (figure 5). This effect was more pronounced for chitosan, most likely as this was less porous than PHB and thicker than PCL. The reduction in cumulative drug release at 60 min was statistically significant for both double-coated chitosan and double-coated PHB samples compared to uncoated ones. In addition, difference in cumulative drug release was statistically significant at 120 min for double-coated chitosan and uncoated samples.

The experimental data of the cumulative drug release were fitted using the Korsemeyer-Peppas's equation, which is one of the release models that can be applied to mesoporous materials [18]. This showed that the diffusion

mechanism was overall altered by the presence of polymer coatings, as the deviation from Fick diffusion ($n = 0.5$) was more significant. As can be seen from the equations reported in figures 3 and 4, the release exponent (n) had values ranging from 0.71 to 0.78 for polymer-coated samples, while it was equal to 0.66 for uncoated nanotubes. Mathematical models to describe drug release kinetics are important tools to understand and control the drug release rate and thus achieve the optimal dosage within the time frame required by a specific therapy [32]. A zero-order release kinetics is often desirable to release drug at a uniform and constant rate [15]. The release exponent closer to 1 observed in this work for the polymer-coated samples seems indicating that use of polymer coatings can be an effective way to achieve zero-order kinetics, as confirmed by others as well [21]. Finally, future work with *in vitro* studies should be carried out to assess cell responses for both uncoated and coated substrates and investigate the efficacy of TNTs-released pen-strep in reducing bacteria proliferation.

5. Conclusion

The combination of surface modification and local drug delivery have the potential to create drug-releasing bone implants able to simultaneously address major post-surgery challenges, i.e. poor osseointegration, inflammatory responses and bacterial infections. Ti64 samples with a dual-scale surface topography were obtained combining SLM and electrochemical anodization. TNTs with a diameter of around 70 nm were loaded with a solution of penicillin-streptomycin, which was released *in vitro* over four hours, displaying a significant initial burst release of 90% in 120 min. For the first time on dual-scale topography samples, we investigated the effect of chitosan, PCL and PHB single and double-layer coatings on drug release. Total drug release time was slightly extended by the presence of coatings, especially for samples double-coated with PCL and PHB (320 min from 240 min). In addition, polymer coatings reduced the initial burst release by 8% (PHB—one layer) to 28% (chitosan—two layers) and altered the overall drug release pattern to be closer to a zero-order, as indicate by fitting with the Korsmeyer-Peppas power law equation. Therefore, the feasibility of using spin coated polymer coatings to control local drug delivery from dual-scale AM implants was demonstrated. Different drug-polymer combinations could be explored in future studies, aiming to extend the drug release and optimize its kinetics.

Acknowledgments

3D printing was completed at the Additive Manufacturing Innovation Centre at Mohawk Collage (Hamilton, ON). SEM imaging using the JEOL microscope was performed at the Canadian Centre for Electron Microscopy (Hamilton, ON). Laser profilometry and SEM imaging with the Zeiss microscope were carried out at the facility 'Servizio di Analisi Microstrutturali dei Materiali' (SAMM) at Politecnico di Milano (Milan, Italy). The authors would like to thank Prof. Gabriele Candiani for the support and help for the drug release tests.

Data availability statement

The data that support the findings of this study are available upon reasonable request from the authors.

Conflict of interest

The authors declare no potential conflict of interest.

ORCID iDs

Chiara Micheletti https://orcid.org/0000-0001-5823-6399
Raffaella Suriano https://orcid.org/0000-0002-7448-359X
Kathryn Grandfield https://orcid.org/0000-0002-0188-9580
Stefano Turri https://orcid.org/0000-0001-8996-0603

References

[1] Liu X, Chu P K and Ding C 2004 Surface modification of titanium, titanium alloys, and related materials for biomedical applications *Mater. Sci. Eng. R Reports* **47** 49–121
[2] Hanawa T 1991 Titanium and its oxide film: a substrate for formation of apatite *The Bone-Biomaterial Interface* ed J E Davies (Toronto, Canada: University of Toronto Press) pp 49–619781442671508
[3] Van N R 1987 Titanium: the implant material of today *J. Mater. Sci.* **22** 3801–11

[4] Albrektsson T, Brånemark P-I, Hansson H-A and Lindström J 1981 Osseointegrated titanium implants: requirements for ensuring a long-lasting, direct bone-to-implant anchorage in man *Acta Orthop. Scand.* **52** 155–70
[5] Puleo D A and Nanci A 1999 Understanding and controlling the bone implant-interface *Biomaterials* **20** 2311–21
[6] Davies J E, Mendes V C, Ko J C H and Ajami E 2014 Topographic scale-range synergy at the functional bone/implant interface *Biomaterials* **35** 25–35
[7] Bauer S, Schmuki P, von der Mark K and Park J 2013 Engineering biocompatible implant surfaces. Part I: materials and surfaces *Prog. Mater. Sci.* **58** 261–326
[8] Pyka G *et al* 2012 Surface modification of Ti6Al4V open porous structures produced by additive manufacturing *Adv. Eng. Mater.* **14** 363–70
[9] Gu D and Shen Y 2009 Balling phenomena in direct laser sintering of stainless steel powder: metallurgical mechanisms and control methods *Mater. Des.* **30** 2903–10
[10] Brånemark R, Emanuelsson L, Palmquist A and Thomsen P 2011 Bone response to laser-induced micro- and nano-size titanium surface features *Nanomedicine Nanotechnology, Biol. Med.* **7** 220–7
[11] Roy P, Berger S and Schmuki P 2011 TiO_2 nanotubes: synthesis and applications *Angew. Chemie - Int. Ed.* **50** 2904–39
[12] Oh S, Daraio C, Chen L-H, Pisanic T R, Finõnes R R and Jin S 2006 Significantly accelerated osteoblast cell growth on aligned TiO_2 nanotubes *J. Biomed. Mater. Res.* **78A** 97–103
[13] Bjursten L M, Rasmusson L, Oh S, Smith G C, Brammer K S and Jin S 2010 Titanium dioxide nanotubes enhance bone bonding *in vivo* *J. Biomed. Mater. Res.* **92A** 1218–24
[14] Gulati K, Aw M S, Findlay D and Losic D 2012 Local drug delivery to the bone by drug-releasing implants: perspectives of nano-engineered titania nanotube arrays *Ther. Deliv.* **3** 857–73
[15] Losic D, Aw M S, Santos A, Gulati K and Bariana M 2015 Titania nanotube arrays for local drug delivery: recent advances and perspectives *Expert Opin. Drug Deliv.* **12** 103–27
[16] Buchholz H W, Elson R A, Engelbrecht E, Lodenkämper H, Röttger J and Siegel A 1981 Management of deep infection of total hip replacement *J. Bone Jt. Surg.* **63** 342–53
[17] Jain A K and Panchagnula R 2000 Skeletal drug delivery systems *Int. J. Pharm.* **206** 1–12
[18] Aw M S, Kurian M and Losic D 2014 Non-eroding drug-releasing implants with ordered nanoporous and nanotubular structures: concepts for controlling drug release *Biomater. Sci.* **2** 10–34
[19] Khudhair D *et al* 2016 Anodization parameters influencing the morphology and electrical properties of TiO_2 nanotubes for living cell interfacing and investigations *Mater. Sci. Eng.* C **59** 1125–42
[20] Aw M S, Gulati K and Losic D 2011 Controlling drug release from titania nanotube arrays using polymer nanocarriers and biopolymer coating *J. Biomater. Nanobiotechnol.* **2** 477–84
[21] Gulati K, Ramakrishnan S, Aw M S, Atkins G J, Findlay D M and Losic D 2012 Biocompatible polymer coating of titania nanotube arrays for improved drug elution and osteoblast adhesion *Acta Biomater.* **8** 449–56
[22] Kumeria T *et al* 2015 Advanced biopolymer-coated drug-releasing titania nanotubes (TNTs) implants with simultaneously enhanced osteoblast adhesion and antibacterial properties *Colloids Surfaces B Biointerfaces* **130** 255–63
[23] Gulati K *et al* 2017 Anodized 3D-printed titanium implants with dual micro- and nano-scale topography promote interaction with human osteoblasts and osteocyte-like cells *J. Tissue Eng. Regen. Med.* **11** 3313–25
[24] Maher S *et al* 2016 *3D printed titanium implants with nano-engineered surface titania nanotubes for localized drug delivery Chemeca 2016: Chemical Engineering-Regeneration, Recovery and Reinvention* p 65
[25] Jia H and Kerr L L 2013 Sustained ibuprofen release using composite poly(lactic-co-glycolic acid)/titanium dioxide nanotubes from Ti implant surface *J. Pharm. Sci.* **102** 2341–8
[26] Micheletti C *et al* 2020 Ti-5Al-5Mo-5V-3Cr bone implants with dual-scale topography: a promising alternative to Ti-6Al-4V *Nanotechnology* **31** 235101
[27] Wenzel R N 1936 Resistance of solid surfaces to wetting by water *Ind. Eng. Chem.* **28** 988–94
[28] Rupp F *et al* 2014 A review on the wettability of dental implant surfaces I: theoretical and experimental aspects *Acta Biomater.* **10** 2894–906
[29] Korsmeyer R W, Gurny R, Doelker E, Buri P and Peppas N A 1983 Mechanisms of solute release from porous hydrophilic polymers *Int. J. Pharm.* **15** 25–35
[30] Peppas N A 1985 Analysis of Fickian and non-Fickian drug release from polymers *Pharm. Acta Helv.* **60** 110–1 (PMID: 4011621)
[31] Gulati K, Santos A, Findlay D and Losic D 2015 Optimizing anodization conditions for the growth of titania nanotubes on curved surfaces *J. Phys. Chem.* C **119** 16033–45
[32] Costa P and Sousa Lobo J M 2001 Modeling and comparison of dissolution profiles *Eur. J. Pharm. Sci.* **13** 123–33
[33] Ventola C L 2014 Medical applications for 3D printing: current and projected uses *P&T* **39** 704–11 (PMID: 25336867)
[34] Bandyopadhyay A, Bose S and Das S 2015 3D printing of biomaterials *MRS Bull.* **40** 108–14
[35] Simovic S, Losic D and Vasilev K 2010 Controlled drug release from porous materials by plasma polymer deposition *Chem. Commun.* **46** 1317–9
[36] Norrman K and Larsen N B 2005 Studies of spin-coated polymer films *Annu. Reports Prog. Chem. Sect.* C **101** 174–201
[37] Lawrence C J 1988 The mechanics of spin coating of polymer films *Phys. Fluids* **31** 2786–95
[38] Mondal D, Griffith M and Venkatraman S S 2016 Polycaprolactone-based biomaterials for tissue engineering and drug delivery: current scenario and challenges *Int. J. Polym. Mater. Polym. Biomater.* **65** 255–65
[39] Hazer D B, Kiliçay E and Hazer B 2012 Poly(3-hydroxyalkanoate)s: diversification and biomedical applications. A state of the art review *Mater. Sci. Eng.* C **32** 637–47
[40] Hamlekhan A *et al* 2015 Fabrication of drug eluting implants: study of drug release mechanism from titanium dioxide nanotubes *J. Phys. D: Appl. Phys.* **48** 275401
[41] Armentano I, Dottori M, Fortunati E, Mattioli S and Kenny J M 2010 Biodegradable polymer matrix nanocomposites for tissue engineering: a review *Polym. Degrad. Stab.* **95** 2126–46
[42] Scholz C 2000 Poly(*β*-hydroxyalkanoates) as potential biomedical materials: an overview,' in Polymers from Renewable Resources *ACS Sympos.* ed C Scholz and R A Gross vol 764 (Washington, DC: American Chemical Society) pp 328–34
[43] Najdahmadi A, Lakey J R and Botvinick E 2018 Structural characteristics and diffusion coefficient of alginate hydrogels used for cell based drug delivery *MRS Adv.* **3** 2399–408